UNIVERSITY OF UTAH
DEPARTMENT OF PHYSICS
SALT LAKE CITY, UTAH 84112

TECHNICAL REPORT

to

ADVANCED RESEARCH PROJECT AGENCY

Principal Investigators

John W. DeFord (Phone 801 322-6971)
Associate Professor of Physics
Owen W. Johnson (Phone 801 322-7166)
Associate Professor of Physics
Adjunct Associate Professor of Material Science and Engineering
Franz Rosenberger
Research Assistant Professor and Director of Crystal Growth Laboratory

Title

ELECTRONIC AND RADIATION DAMAGE PROPERTIES OF RUTILE

Period:	1 year
Date:	June 1, 1970 to May 31, 1971
Amount:	$111,000

Grant No. DAHC15-70-G-13

Contractor	Defense Supply Service - Washington
Project Monitor	Dr. O. C. Trulson Deputy Director for Materials Sciences Advanced Research Projects Agency Washington, D. C. 20301

Sponsored By

Advanced Research Projects Agency

ARPA Order No. 1610

In the first six months of this project we have concentrated our effort in the following areas:

I. Group Development

We have devoted considerable effort to recruiting and organizing our research group for this project. We have added the two postdoctoral fellows called for in our proposal. They are Dr. John Shaner and Dr. Richard Brandt. We are extremely fortunate to have been able to recruit these people, as both are very outstanding young physicists. A brief summary of their qualifications follows.

Dr. Shaner received his B.S. from MIT in 1964 and his Ph.D. from the University of California at Berkeley in 1969 under Professor E. L. Hahn. He held a postdoctoral position at Berkeley from 1969 until August 1970 when he joined our group.

He has worked in ultrasonic attenuation in addition to the fields already represented by his publications:

1) "Mossbauer Studies of Spin Flip in Antiferromagnetic Hematite", (with N. Blum, A. J. Freeman and L. Grodzins) J. Appl. Phys. 36, 1136 (1965).

2) "Shock Induced Demagnetization of YIG", (with E. B. Royce) J. Appl. Phys. 39, 492 (1968).

3) "Zero Field Free Precession Measurements of the Hyperfine Interaction in Cs^{133} Vapor", (with S. A. Miller and E. L. Hahn) Bull. Am. Phys. Soc. 13, 398 (1968).

4) "Cyclotron Echoes in a Weakly Ionized Cesium Plasma", (with E. L. Hahn) J. Appl. Phys. 41, 838 (1970).

He came enthusiastically recommended by Professor Hahn and many other physicists who have had the opportunity to observe him. Since arriving he

has thoroughly lived up to our expectations.

Dr. Brandt received his B.S. from Cal Tech in 1962 and his Ph.D. from the University of Illinois in 1967 under Professor Fred Brown. From 1967 to the present he has been at Lincoln Labs working primarily on far infrared spectroscopy. He will join us early in 1971.

His publications include:

1) "Etching on High Purity Zinc", (with K. H. Adams and T. Vreeland, Jr) J. Appl. Phys. 34, 587 (1963).

2) "Dislocations and Etch Figures of High Purity Zinc", (with K. H. Adams and T. Vreeland, Jr.) J. Appl. Phys. 34, 591 (1963).

3) "Infrared Absorption and Vibronic Structure due to Localized Polarons in the Silver Halides", (with F. C. Brown) in Localized Excitations in Solids, edited by R. F. Wallis (Plenum Press, Inc., New York, 1968).

4) "Polaron Zeeman Effect in AgBr", (with D. M. Larsen, P. P. Crooker and G. B. Wright) Phys. Rev. Letters 23, 240 (1969).

5) "Induced Infrared Absorption due to Bound Charge in the Silver Halides", (with F. C. Brown) Phys. Rev. 181, 1241 (1969).

6) "A Beam Condenser for Infrared Spectrophotometers", Appl. Optics 8, 315 (1969).

7) "Polaron Zeeman Effects in the Silver Halides", (with D. M. Larsen and D. R. Cohn) Proceedings of the 10th International Conference on Physics of Semiconductors, Cambridge, August 1970. to be published.

Dr. Brandt was enthusiastically recommended by many physicists including Professors Mauer and Brown at Illinois. However, the strongest recommendation of all is that he turned down a position as Assistant Professor at the University of Illinois to join our group.

We anticipate Dr. Brandt being a great asset to the group, particularly

since he is an established expert in far infrared spectroscopy, and has had considerable experience in research on wide-gap semiconductors.

In addition to Brandt and Shaner whom we have brought into the Department we have enlisted the help of some people already on the staff. Professor Frank Harris has become interested in an empirical band structure calculation on rutile and has donated the services of one of his postdoc's to the calculation--under his supervision. Professor Harris has an international reputation as a theorist and we are very pleased to have his help. Results of this calculation should be very helpful in interpreting electronic measurements.

We also have two graduate students--one working on photoconductivity and one on crystal growth.

II. Crystal Growth

A good part of the crystal growth program during the first six months under this grant has involved a comprehensive literature study of potential crystal growth techniques for rutile and the physical chemistry of certain titanium compounds which might be used as starting materials for the preparation of ultrapure TiO_2 in later stages. Consequently detailed plans for the crystal growth and purification equipment as well as consecutive goals in the procedures were worked out. The crystal growth furnace, a novel development, has been built and tested already. First growth runs will be performed within the next two months.

III. Dielectric Loss Measurements

Current status of this part of the project is summarized in Appendix I, which is a preprint of a paper to be submitted shortly.

IV Dielectric Loss Analysis

This aspect of the program has turned out to be a rather formidable

problem and has required a substantial effort. The problem is best handled in two steps; the dielectric loss and capacitance spectrum are first "inverted" to obtain a resistivity spectrum, which must then be ordered in such a way as to satisfy Poisson's equation. The first part of the procedure has now been reduced to a routine computer analysis and we have made considerable progress in handling the second step; further progress will require knowledge of electron trapping levels, which we expect to obtain from other measurements. The details of the analysis of dielectric loss data are also summarized in Appendix I.

v. Review Paper

Probably because of its unique properties, TiO_2 has attracted a great deal of interest and research is being carried on by investigators in many different disciplines. Because of this, research results are published in a wide variety of journals, many of which are not readily accessible. The extent of the research activity in this field is quite startling; in the past three years, more than 250 technical papers concerning the physical properties of rutile and closely related compounds have been published. We felt it was absolutely essential to thoroughly digest all of this material before proceeding very far on most of our investigations, particularly since some of our group had not previously worked on this material. Any group working in this area, of course, is (or should be) confronted by the same problem. The last comprehensive review paper in this area was published in 1959; a really thorough and critical review is badly needed. We felt we could perform a substantial service to the scientific community by summarizing the results of our extensive literature search and evaluation in the form of a review article. We have already received the blessing of the editors of Reviews of Modern

Physics for this project and are well on our way to completing this work. We have on file virtually all of the significant papers published in this area in the past ten years, have cataloged and cross-referenced these (see attached outline) and have already completed evaluation of many of them. We have begun writing the sections concerning electrical, optical, and mechanical properties, and the phonon spectrum.

This project, in addition to serving a very useful purpose for other workers in the field, has been extremely helpful to us directly, in that it has brought out the importance of several areas of investigation and has suggested several critical experiments which should help to resolve some of the apparent contradictions in the literature. In particular, optical measurements on conduction electrons at low temperatures, far infrared spectroscopy for study of defects and ultrasonic attenuation measurements look very promising (these are discussed in detail in Sec. II).

In addition, we have set up the experimental equipment to do photoconductivity measurements and have made several runs with it. There do not appear to be any serious experimental problems, but the results are very complex and we have not yet achieved sufficient understanding to merit a detailed discussion.

We have nearly completed the experimental set up for photoemission studies but have not yet taken any actual data.

Our work on devices thus far has consisted of formulating some specific configurations we would like to investigate. Potential problems associated with fabrication of these devices have been discussed with Dr. Robert Huber of General Instruments, and arrangements for production of the devices by General Instruments have been completed.

Working Outline for the Rutile Review Paper

I. Crystal Growth and Preparation

- a. Structure and Stoichiometry
- b. Growth
- c. Purification
- d. Sample Preparation

II. Electrical Properties

- a. Conductivity
- b. Hall Effect Measurements
- c. Photoconductivity
- d. Piezo-resistance
- e. Dielectric Loss
- f. Ultrasonic Attenuation

III. Thermal Properties

- a. Thermal Conductivity
- b. Thermoelectric Effects
- c. Specific Heat
- d. Anharmonic Effects

IV. Optical Properties

- a. Optical Absorption and Reflection
  1. Ultraviolet
  2. Visible
  3. Infrared
- b. Modulation Spectroscopy
- c. Dielectric Function
- d. Raman Scattering
- e. Photoemission
- f. Thermal Emission and Related Effects

V. Magnetic Properties

a. Susceptibility

b. Nuclear Magnetic Resonance and Mössbauer Effect

c. Electron Paramagnetic Resonance

d. Maser Action

VI. Electronic Structure

a. Intrinsic Band Structure

b. Defect and Impurity Levels

VII. Phonon Spectrum

VIII. Intrinsic Defects (Ti or O)

IX. Impurities (Defects other than Ti or O)

X. Mechanical Properties

a. Internal Friction

b. Elasticity Experiments

XI. Radiation Damage

XII. High Pressure Properties

APPENDIX I

Dielectric Loss Mechanism in Rutile (TiO_2)*

O. W. Johnson and John W. DeFord
Department of Physics, University of Utah
Salt Lake City, Utah 84112

Sverre Myhra
Department of Physics, University of Queensland
Brisbane, Australia

A new mechanism to account for the anomalously large dielectric loss and apparent dielectric constant frequently observed in TiO_2 is presented, which appears to agree well with experiment. The mechanism involves field-induced donor migration, resulting in a large decrease in electronic resistivity in part of the crystal. Experimental results on a variety of crystals are discussed, and the influence of electrode materials, surface condition, heat treatment and ambient is analyzed. A method for numerically calculating the resistivity profile of such a crystal from dielectric loss data is described. Results indicative of room temperature p-type conductivity, and a voltage-induced conduction process are presented.

---

*Work supported by ARPA, Grant No. DAHC 15 G 13.

I. Introduction

Previous dielectric loss studies in rutile[1-8] have yielded results which have been interpreted to imply anomalously large frequency dependent dielectric constants ranging as high as 10^4, both for oxidized crystals and slightly reduced crystals, in which two terminal dc resistance measurements indicate a resistivity $\sim 10^{13}$ ohm-cm for oxidized, and from 10^8 to 10^{12} ohm-cm for reduced crystals. In contrast, microwave measurements[1,10] have consistently yielded $\epsilon \approx 173\ \epsilon_o$ ($\epsilon_o = 8.85 \times 10^{-12}$ in MKS units) in the c-axis direction. The anomalously large apparent dielectric constants have generally been accompanied by dielectric loss peaks (D = 0.5 or more, even in heavily oxidized crystals), typically in the frequency range from 10^3 to 10^4 Hz. A layer of material of resistivity ρ will exhibit large electronic dissipation only at frequencies less than $\sim 1/(2\pi\rho\epsilon)$.[9] Assuming $\epsilon \approx 170\ \epsilon_o$ and $\rho \approx 10^{13}\ \Omega$ cm, significant electronic dissipation should be observed only below $\sim 10^{-3}$ Hz. Thus, if the loss peaks are electronic in origin large dissipation in the kilocycle range would require either material with ρ of 10^6 or $10^7\ \Omega$ cm, or a very large and strongly frequency dependent dielectric constant. Mechanisms to account for these results have generally involved a "depletion layer" (i.e., a layer in which the "normal" concentration of conduction electrons has been reduced), induced by the metal electrodes in contact with the crystal, or an enhancement of the dielectric constant due to the presence of conduction electrons. As we shall show, the first mechanism--by itself--will not produce the observed dielectric loss peaks. The second mechanism is readily ruled out by calculating the contribution of conduction electrons to the real part of the dielectric constant.[11] It is many orders of magnitude too small to account for the observed effects. Motion of any other charged species

present could contribute to dielectric loss, but none of the known defects or impurities in rutile diffuse rapidly enough at room temperature to contribute significantly. Other loss mechanisms, such as dipolar reorientation, motion of charge dislocations, loss due to conductive inclusions, etc., also appear to be ruled out by the known properties of the crystal.

II. Analysis of Electronic Dielectric Loss

In the absence of any other plausible loss mechanism, we have attempted to account for the observed behavior on the basis of changes in bulk resistivity of the crystal, induced by contact with the electrode material. We assume that none of the bulk parameters of the crystal, except for the resistivity, are changed by the presence of the electrodes, and that the thickness of the crystal is small compared to its lateral dimensions. The required resistivity spectrum can be derived from the experimental measurements in a fairly straightforward way. By "resistivity spectrum" we mean the total thickness of layers having resistivity ρ_i. The analysis gives no information as to the "resistivity profile", i.e., the relative position of the layers. The resistivity profile can in principle be obtained by requiring that the layers be arranged to satisfy Poisson's equation with appropriate boundary conditions.

We can derive the resistivity spectrum as follows: the complex impedance z of a crystal of thickness ℓ (assuming planar geometry) is

$$\tilde{z} = \int_0^{\ell} d\tilde{z} = \int_0^{\ell} \left[\frac{\rho(x) - i\rho^2(x)\omega\varepsilon}{\rho^2(x)\omega^2\varepsilon^2 + 1} \right] dx$$

$$= \ell \int_0^{1} \frac{\rho(\theta) - i\rho^2(\theta)\omega\varepsilon}{\rho^2(\theta)\omega^2\varepsilon^2 + 1} \, d\theta \qquad (1)$$

where ω is the angular frequency. The experimentally measured parameters are the series equivalent capacitance C and the dissipation D, given by

$$C = -\frac{1}{\omega \mathrm{Im}(\tilde{z})} \quad \text{and} \quad D = \frac{\mathrm{Re}(\tilde{z})}{\mathrm{Im}(\tilde{z})}$$

Thus, $\tilde{z}(\omega)$ may be determined from the experimental parameters. Our problem is to solve the integral equation (1) for ρ. There are several possible approaches to the problem, but all involve approximating the integral by a sum:

$$\tilde{z}(\omega_j) \approx \ell \sum_k \frac{\rho_k - i\rho_k^2 \omega_j \epsilon}{(\rho_k \omega_j \epsilon)^2 + 1} \theta_k = \ell \sum_k \tilde{a}_{kj} \theta_k \qquad (2)$$

where ρ_k is the average resistivity of the k^{th} layer, of thickness $\ell\theta_k$.

In this form it is obvious that the ordering of the layers is immaterial and hence that only the resistivity spectrum can be determined in this fashion. One possible approach at this point is simply to assume a set of ρ's. This determines the $\tilde{a}_{kj}$ in Eq. (2). If n ρ's are chosen we can then use (n-1) data points to get (n-1) equations in the n unknowns, θ_k. By then imposing the condition

$$\Sigma\theta_k = 1$$

we get a system of n equations in n unknowns which can be solved exactly. Unfortunately the exact solutions obtained in this way are generally non-physical (some of the θ_k turn out to be negative), due to the approximations inherent in the technique and small inaccuracies in the experimental data. Thus, a somewhat more sophisticated treatment is required.

The first improvement is to use a form of least squares fit rather than attempting an exact solution to an inexact problem. Instead of $\tilde{z}(\omega)$ it is convenient to use the dissipation $D(\omega)$ (either $C(\omega)$ or $D(\omega)$

may be used since they are related by Kramers-Kronig equations). Approximating the integrals by sums we have

$$D(\omega) = \frac{\sum_{k=1}^{n} \frac{\rho_k \theta_k}{(\rho_k \omega \epsilon)^2 + 1}}{\sum_{k=1}^{n} \frac{\rho_k^2 \theta_k \epsilon \omega}{(\rho_k \omega \epsilon)^2 + 1}} \qquad (3)$$

where we now restrict the fractional thicknesses, θ_k, to non-negative values; n is the assumed number of layers. A reasonably good ($\sim 2\%$) fit to the experimental $D(\omega)$ can be found by trying various ρ and θ choices, plotting out the resulting theoretical curves (calculated from Eq. (3)), and adjusting the ρ_k and θ_k to get the best fit. This method works reasonably well, because a given resistivity layer affects D only over a fairly narrow frequency range[9] and hence the corrections in ρ can be made more or less systematically. Unfortunately, it is tedious, time consuming, and not suitable for routine analysis. Hence we have developed a more systematic approach using the 1108 computer. This approach is described in Appendix A. It leads to a resistivity spectrum which gives the best least squares fit between calculated and experimental dissipation curves.

Assuming the resistivity spectrum is now known, the corresponding conduction electron density is determined, in terms of the electron mobility μ. Knowledge of the density of states in the conduction band would then permit calculation of the position of the bottom of the conduction band, E, relative to the Fermi level, E_F. We now formulate the problem of ordering the layers to obtain the resistivity profile.

Poisson's equation may be written

$$\nabla^2\phi = -\frac{\bar{\rho}}{\epsilon} = -\frac{e}{\epsilon}\left[N_+ - n_T - n_c\right] \qquad (4)$$

where ϕ is the electrostatic potential, $\bar{\rho}$ is the net charge density, $e = 1.6\times10^{-19}$ coul., n_T and n_c are the densities of electrons in traps and the conduction band, respectively, and eN_+ is the net positive charge density, due to impurities, defects, etc. We assume that before application of electrodes, ϕ is constant through the crystal, so that $N_+ = n_T + n_c$. We assume throughout that E_F is well above the valence band so that hole density can be ignored (although there is some evidence that this assumption may not be valid in certain cases, as discussed in the next section). N_+ will consist of various substitutional and interstitial species, some of which apparently are mobile at temperatures of $\sim 300^{\circ}C$; it is convenient to write

$$N_+ = N_F + \sum_I Z_I N_I$$

where N_F includes all immobile ions, and eZ_I is the charge of the I^{th} mobile ion species, with density N_I.

In the absence of space charge, E_c is just the binding energy of a conduction electron to the crystal, and is fixed relative to the vacuum level. Space charge layers in the crystal result in a shift of the potential energy of an electron in the conduction band in the interior of the crystal; thus, in general E_c will be a function of position, and it is clear that

$$E_c(x) = -e\phi(x) + \gamma$$

where γ is a constant which depends on our choice of zero of potential.

It is also clear that E_c at the surface of the crystal is constant relative to the vacuum level in the absence of space charge external to the crystal.

We may write expressions for n_c and n_T in terms of E_c and the Fermi energy E_F:

$$n_c = \int_{E_c}^{\infty} \frac{D(E)dE}{e^{\beta(E-E_F)} + 1} \approx \frac{n_o}{e^{\beta(E_c-E_F)} + 1}$$

$$n_T = \sum_i \frac{n_i}{e^{\beta(E_i-E_F)} + 1}$$

where $D(E)$ is the density of states in the conduction band (for which we use the usual approximation of an effective density of states n_o located at E_c), $\beta = 1/kT$, and n_i is the density of traps with trapping energy E_i.

Thus Eq. 4 becomes

$$\frac{d^2E_c}{d_x^2} = \frac{e^2}{\epsilon}\left[N_F + \sum_I Z_I N_I - n_T - n_c\right] \qquad (5)$$

Next consider the situation with electrodes applied. At equilibrium, the Fermi level will be constant throughout the system. If mobile ions are present, a similar condition must be satisfied for the ions as well--that is, the chemical potential of each mobile species must be constant throughout the system. Before the electrodes are applied we have the situation shown in Fig. 1A.

When the electrodes are applied, charge will flow until E_F is constant throughout the system. Since the density of states is much higher in the metal than in the rutile, the Fermi level in the metal will not change appreciably. Furthermore, the resulting space charge in the metal will be confined to a very thin layer ($\lesssim 10^{-7}$ cm) adjacent

to the rutile; hence, E_c at the surface of the rutile is essentially unchanged by the presence of the electrodes. There are three possibilities: 1) The Fermi level is initially higher in the metal than in the rutile, i.e., the work function of the rutile is > the work function of the metal. (We refer throughout to the thermodynamic work function, the difference between the vacuum level and E_c.) 2) The Fermi level is initially lower in the metal than in the rutile. 3) The Fermi level is initially the same in both materials. In case 1), electrons will flow from the metal to the rutile raising E_F in the rutile, resulting in a net positive charge in the metal at the interface and a net negative charge in the rutile. Due to the planar geometry we can use Gauss's Law to determine the fields and energies involved. We can, without significant error, treat the metal space charge as a charge layer $\sigma+$ at x = o, the rutile-metal interface. Then the change in electrostatic potential, $\Delta\phi$, at a depth x in the rutile is given by

$$\Delta\phi = -\int_{o-}^{x} E(x')dx' = -\frac{1}{\epsilon}\int_{o-}^{x}\left[\sigma+ -\int_{o}^{x'}\overline{\rho}(x'')dx''\right]dx'$$

where $\overline{\rho}$ is the net charge density in the rutile, and E is the resulting electric field. Thus, $\Delta\phi \to o$ as $x \to o$, so that the energy levels at the surface of the rutile are unchanged by application of electrodes, as previously noted. Note also that $\int_{o}^{x}\overline{\rho}(x)\,dx \to \sigma+$ as $x \to \infty$, in order to maintain overall charge neutrality. The electron energy levels in the interior are shifted by the electrode-induced space charge by

$$\Delta E_c = (e\Delta\phi) = \frac{e}{\epsilon}\int_{o-}^{x}\left[\sigma_+ - \int_{o}^{x'}\overline{\rho}(x'')dx''\right]dx'.$$

Hence, the resulting configuration is as indicated in Fib. 1B. The thickness of the space charge layer can be calculated numerically from

the initial difference in Fermi levels, if the trap density is known and there is no positive ion migration. For physically reasonable differences in work function, the calculated thickness of the layer is always < 1μ, even in the absence of electron traps (traps reduce the thickness). Hence, the effect of the electrodes, in the absence of ion motion, is to induce a very thin (typical sample thickness is ~ 500μ) conducting layer near the surface, leaving the bulk of the crystal unchanged.

Curve A in Fig. 2 presents the results obtained from a numerical integration of Eq. (5), assuming $E_c - E_F$ before electrodes were applied was ~ 1.5 eV at room temperature, that conduction band density of states could be represented by an effective density, n_o of $10^{20}/cm^3$ at E_c, and that the difference in work functions, $(W_R - W_M) \geq 1.35$ eV. We further assumed that there were no electron trapping levels above E_F; this is probably not the case, but failure of this assumption would not result in major changes in the calculated parameters. Our results are not particularly sensitive to our choice of n_o, either, except for the calculated values of donor density discussed below, which must be considered rough estimates. For the assumed parameters, D is negligible and C constant over our frequency range, as indicated by Curves A of Fig. 3.

The question of possible ion motion must now be considered. It is readily shown that the effect of a field E on a charged impurity is to produce a drift velocity

$$v_d \approx \frac{ZeE}{kT} D$$

where D is the thermal diffusion coefficient, and Ze is the ion charge. While precise values of D are not available for any of the donor impurities

(except Li,[12] which is probably not present in appreciable concentrations) reasonable estimates indicate that many interstitial ions should move significant distances at temperatures of $\sim 300^{\circ}C$, in the presence of a field, even though significant thermal diffusion is not observed except at substantially higher temperatures. In particular, H^{+} is certainly mobile in this range (as discussed below) and other species with ionic radius $\lesssim 0.70\text{Å}$, including Ti^{4+}, may move to a lesser extent.[13,14]

Thus, we assume that there are positive ions present which are mobile in the presence of an electric field, at least at temperatures of the order of 200 - 300°C, as indicated by experimental results described in Sec III. In the electron space charge region these ions are subjected to a large electric field ($> 10^{3}$V/cm), driving them away from the electrodes, due to the combined effect of the net positive charge at the interface and the distributed rutile space charge layer. This will tend to remove positive ions from a layer beneath the electrodes until, at equilibrium, the ion concentration gradient just balances the electric field.

It is straightforward to show that at equilibrium, the concentration of ions is given by:

$$N_I(x) = N_o \exp\left\{\left[\left(\frac{Z_I e}{kT}\right)\left[\phi_o - \phi(x)\right]\right]\right\}$$

where $Z_I e$ is the charge of the ion, N_o and ϕ_o are the values at $x = 0$, and $\phi(x)$ is the electrostatic potential at x. (After ion migration--the change in ion distribution alters ϕ from the value previously calculated, of course.) It follows that the fractional change per unit distance is given by:

$$\frac{1}{N}\frac{dN}{dx} = \frac{ZeE}{kT}$$

where $E = -d\phi/dx$. Thus, the concentration will change with a "characteristic

length" given by

$$\Delta x \approx \frac{kT}{ZeE} .$$

A space charge layer containing 10^{10} electrons/cm^2 results in $\Delta x \approx 1\mu$. As shown below, a typical space charge layer has roughly 10^{12} electrons/cm^2; hence, the concentration will change over a distance which is small compared to the typical sample thickness, resulting in an equilibrium positive ion distribution which is essentially a step function. Note that it is possible for this depletion layer to be much thicker than the original space charge layer, since the region of high field "migrates" into the crystal as the positive ions are displaced.

It is readily seen that the central region of the crystal is in a state of almost exact charge neutrality, since any significant departure from neutrality results in further ion migration and hence does not represent equilibrium. An electric field is possible only in the narrow region where the positive ion distribution is changing, and in the ion depletion layer. The exact configuration may be obtained from Eq. (5) with appropriate substitutions for the various change density terms, and with the boundry condition on $E_c(0)$ fixed in terms of the relative work functions of the rutile and the electrode. A subsidiary condition on the total number of mobile ions must be applied to obtain a unique solution to this equation. In the case where only ions already in the crystal are involved, the condition is simply that the total number of ions in the crystal must be constant. If donor impurities may diffuse in from the electrodes or the ambient, the final concentration is fixed from thermodynamic considerations and represents the solubility limit for the given experimental conditions (this point is discussed in detail in the next section). For the assumed values of the parameters of the

specimen described above, the result of numerical integration of Eq. (5) for a temperature of 350°C is shown in Fig. 2, Curve B. For this calculation, an initial density of mobile ions of $4 \times 10^{14}/cm^3$ was assumed, and it was assumed that no donor impurities diffused in from the ambient. This density is probably too low but essentially indistinguishable results obtain with a higher density of mobile ions, so long as they are compensated by electron trapping states, as would be required to produce the high initial resistivity. For the assumed initial density, equilibrium at 350°C requires essentially complete depletion to a depth of $\sim 6\mu$, then very rapid increase to a constant value of $\sim 4.1 \times 10^{14}/cm^3$.

The behavior indicated in Fig. 2 is a general feature of all of our calculations; it turns out that for any reasonable choice of parameters and for thicknesses of $\gtrsim 100\mu$, there is always a broad central region of essential charge neutrality and uniform ion density. Even small net charge densities ($\sim 10^{10}/cm^3$) quickly cause E_c to diverge beyond physically realizable limits.

When the specimen is quenched, the ion distribution will presumably be "frozen in" (we assume, as indicated by experiment, that the ions are relatively immobile at room temperature), whereas the electron distribution changes to re-establish a constant E_F. However, it must be recognized that the electron concentration near the center of the specimen remains essentially at the value established at the annealing temperature, in order to preserve charge neutrality, as discussed above. This is the crucial point in our analysis, since this requires that the quantity $[(E_c - E_F)/kT]_{L/2}$ be the same before and after quenching to room temperature, resulting in a substantial lowering of $E_c(L/2)$. (Note that the presence of unfilled electron traps would reduce the magnitude of the effect but would

not alter the essential conclusions of the analysis.) Again solving Eq. (5) for our assumed parameters, but with the ion distribution calculated in Curve B held fixed, results in Curve C of Fig. 2. This result is rather surprising; we see that the redistribution of the positive ions has resulted in a wide region of relatively low resistivity in the interior, with a thin layer of high resistivity material under the electrodes. As will be seen in the following section, this is precisely the type of resistivity profile required to account for the experimental data. The calculated values of C and D for this specimen are shown as Curves B, Fig. 3. The upward curvature of $E_c(x)$, moving from the interior toward the surface, results from a very slight departure from charge neutrality (electron deficiency) in the center; this is the only conduction band configuration which converges to the correct value at the surface, with the calculated positive charge distribution. The resulting high resistivity layer (at $x \sim 10\mu$ in Fig. 2C) accounts, of course, for the high apparent dc resistivity. Capacitance measurements on this sample would yield an anomalously high apparent dielectric constant, approximately in the ratio of the sample thickness to the thickness of the insulating layer.

In practice, we believe that this situation usually prevails, due to heat treatments made in the application of the electrodes or other steps in the preparation of the specimen. We suspect also that this phenomenon is not confined to rutile but rather may occur in a wide class of materials. Note that the only requirements are a work function greater than that of the electrodes and a positive ion which is mobile under an electric field at elevated temperature, but not at room temperature.

In general, satisfactory treatment of Eq. (5) requires detailed knowledge of trapping levels (which have been ignored at present), as

well as precise values of such parameters as n_o. These calculations are presented solely for the purpose of demonstrating that the model leads to qualitatively good agreement with typical experimental results to be presented in the next section, for physically reasonable choices of parameters.

If the electrode work function is larger than the rutile work function, electrons will flow from the rutile to the metal until the Fermi level is constant throughout. This will result in an $(E_c - E_F)$ which is increased at the surface compared to the value before electrodes were attached. In the middle, $(E_c - E_F)$ will be nearly the same as before, with the width of the transition region being determined by the trap density. If the sample is now heated, any mobile positive ions will be drawn toward the surface, but in this case the electric fields are much smaller, since the number of electrons available to move $(\leq n_c + n_T)$, and hence the net charge density producing the field, is much smaller than before. We have carried out a detailed analysis of this case, following the procedure described above; unless the work function difference is great enough to induce p-type conductivity (which is inconsistent with experimental results except for certain special cases to be discussed in Section III), the changes produced in the ion distribution do not result in increased conductivity anywhere in the crystal. The predicted dissipation and capacitance curves are the same as those in Fig. 2A. The corresponding ion distribution is a slow monotonic decrease from the electrodes toward the center of the crystal; the resistivity is as high or higher everywhere as it was before application of electrodes. The details depend on trap densities and initial ion concentration, but the general result is as outlined. The possibility of p-type conductivity

apparently must be considered in special cases, but cannot usefully be analyzed on the basis of presently available data.

The third case (equal work functions) does not involve space charge layers and, hence, no ion motion is anticipated. There is an additional possibility, that the electrode-rutile interface (or the rutile surface) is charged, due to surface states or defect-induced double layers, but the experimental results seem to be adequately accounted for by the above analysis.

The authors are not aware of any direct measurements of the rutile work function;[15] crude estimates based on previous calculations[16] of electrostatic potential of charged entities in the rutile lattice indicate that a rather large work function should be expected. This is particularly reasonable in view of the large polarizability of rutile. If the assumptions of our model are correct, the existence of the large electronic dissipation peaks observed in this system would indicate a work function significantly greater than the ~ 5 eV which is typical for metals. Our calculations indicate that dielectric loss measurements at frequencies $\leq 10^5$ Hz are insensitive to the exact value of the work function of the electrodes, so long as it is less than that of rutile by ≈ 0.15 eV.

III. Experimental Results

Measurements of C and D have been made on a variety of rutile crystals, subjected to various heat treatments and surface preparations, and with several electrode materials. Measurements reported herein were made on thin disk-shaped crystals, oriented with the c-axis perpendicular to the face of the disk ($c_\perp$). A number of measurements were also made on crystals with the c-axis parallel to the major face of the disk; behavior of these specimens paralleled that of the $c_\perp$ specimens, after allowing for the smaller dielectric constant, except that the temperature-induced changes proceeded more slowly. Typically, equivalent results could be obtained in comparable times by raising the temperature by $\sim 100^{\circ}C$. Sample thickness ranged from 250 to 600μ. Results obtained were not significantly dependent on sample thickness, although longer heat treatments were required to produce the same results in thicker crystals. All measurements were made using a General Radio Model 1615-A bridge. Guard electrodes were used in some cases, but did not appear to affect the measurements, indicating that surface currents were not important. "Pure" crystals from various sources were tested; some differences were observed but there did not appear to be a consistent correlation with source. Doped crystals exhibit quite different and variable behavior, but not enough data is yet available to justify discussion.

The results obtained on various samples and electrode materials were widely variable and obviously dependent on a large number of parameters, not all of which can be adequately controlled or evaluated with presently available crystals. For this reason, it is not possible to present a complete and unified treatment of this complex problem at

present, and no attempt will be made to present data in detail; rather, we simply describe our results qualitatively, drawing conclusions where possible, and indicate areas where additional study is required. Our results are presented in terms of the observed effects of various experimental parameters; in some cases, considerable interpretation is involved and, hence, the conclusions reached must be regarded as tentative.

A. Surface condition

The presence of surface damage results in complicated behavior, which has not been carefully studied. In general, however, the results appear to be consistent with the assumption that surface damage produces a layer of relatively high conductivity in which diffusion of Ti interstitials or other donor centers (discussed below) is inhibited. We were unable to reduce the dielectric loss below ~ 0.1 until after removal of mechanical damage by etching, or after annealing above 1000°C. If mechanical damage results in reducing $(E_c - E_F)$ in the damaged region (for example, by introducing interstitial defects), these observations would be consistent with the analysis in the previous section, with the loss resulting from one of the following mechanisms:

1) In the absence of heat treatments the loss results from the low resistivity damaged surface layer.
2) If the crystal is heated to moderate temperatures the loss results from the induced ion migration described in Sec. II with the damaged layer playing the same role as a metal electrode (i.e., a material with higher initial Fermi level).

High temperature (~1000°C) treatment would allow annealing of these

defects, resulting in a raising of $(E_c - E_F)$ in the damaged layer and reduction of the induced dissipation. Further evidence of the sensitivity of dielectric loss to surface damage is provided by the observation that mechanical polishing of an etched crystal with 0.1μ alumina produced easily detectable changes.

All results described below were obtained on crystals which had been carefully lapped, followed by etching in KOH at $\sim 450^{\circ}C$ to remove at least 25 microns.

B. Electrodes

A variety of electrode materials were applied to the crystals, including Ag lacquer, colloidal graphite, PT and Au pastes (fired @ $\sim 900^{\circ}C$) and evaporated Ti, Al, Ag, and Au. All electrode materials which could be applied at room temperature produced indistinguishable results on a given sample so long as the crystal was not heated after application of electrodes. Loss curves for different samples were widely variable, depending on heat treatment prior to application of electrodes, but were reproducible for a given crystal with different electrodes. The observed dissipation depended in a complicated way on sample purity as well as temperature, ambient, and cooling rate associated with previous heat treatment. The mechanisms responsible for the loss curves observed are not well understood; the only thing that can be said at present is that the loss is definitely electronic in origin. (See Sec. I.) It is worth noting that severe oxidation (i.e., dry O_2 at $1000^{\circ}C$) does not always produce the low loss which would be expected from dc conductivity measurements, suggesting that it is probably possible (at least in some crystals) to produce weak p-type conductivity at room temperature;

failure to observe corresponding dc conductivity probably results from an intrinsic layer induced by the presence of electrodes (due to a transition from n-type to p-type conductivity).

Considerable progress has been made in understanding the nature of the changes which occur when crystals are heat-treated with electrodes in place. It is possible to produce dielectric loss $D < .01$ over the frequency range from 20 to 10^5 cycles (with constant capacitance equal to the calculated value to within 1%, assuming $\epsilon = 173\ \epsilon_o$), or loss peaks anywhere in this frequency range with $D > 10$.

The loss curves observed in crystals heated with electrodes in place can be understood in terms of the model described in the previous section. However, due to differences in sample purity, thermal history, etc., the data are so widely variable (although accurately reproducible for a given crystal, electrode material, and heat treatment) that no useful purpose would be served by a detailed presentation of results. Figure 4 is typical of crystals exhibiting moderately high loss, in that the peak shape is roughly the same in most cases, and the dissipation drops off to ~10% of the peak value at high and low frequencies.

The electrode materials fall into two categories; those which produce irreversible effects on heating and those which do not. By irreversible we mean that the changes in the loss spectrum produced by a given heat treatment (at temperatures of 400°C or less) were not completely reversed by removal of electrodes and reheating to the same temperature. All of the electrode materials listed above, except for Ag and Au, resulted in irreversible changes, all of which were qualitatively similar (although the temperature dependence was different) and could be accounted for by diffusion of donors into the crystal from the

electrode-crystal interface. These materials were also qualitatively different from Au and Ag in that the effect produced by heating did not "saturate" (by "saturate" we mean that increasing the length of the heat treatment produces no further changes) while changes produced by Au and Ag did. For example, a 500μ $c_\perp$ disk with Au or Ag electrodes saturates in $\sim$ 10 hours at 350°C, while irreversible changes associated with Al or Ti electrodes are not observed to saturate after 100 hours. The irreversible changes apparently are produced either by diffusion of material from the electrode (Al, for example) or by chemical reaction of the electrode material with the rutile, resulting in excess Ti which diffuses into the crystal. Al appears to diffuse into the crystal, presumably as a 3^+ interstitial, since the dissipation increases considerably faster in this case than with Ti electrodes. C electrodes were not investigated in detail, except to establish that irreversible effects occurred at 400°C. Pt and Au paste electrodes require firing at elevated temperatures and were abandoned early in the investigation.

The behavior of crystals with evaporated Ag or Au electrodes apparently is quite well accounted for by the model discussed in the preceding section. We find no evidence for contamination of the crystal or reaction with the electrodes, and all changes observed are fully reversible and reproducible for a given crystal, although the observed dissipation depends strongly on the temperature and the ambient atmosphere of the heat treatment (as discussed below), as well as on high temperature heat treatment prior to electrode application and on sample purity. Thus we conclude that the observed dissipation in this case results from the nonuniform distribution of donors, induced by the difference in work function of the electrode and the rutile, as described

in the preceding section. Au and Ag electrodes apparently produce indistinguishable results; our calculations indicate that the difference in work functions for Au and Ag would not result in detectable differences in behavior so long as both are significantly smaller than that for rutile. In fact, we would expect virtually identical results for any nonreactive metal electrode.

Results obtained with Ag lacquer electrodes are similar, though somewhat more variable, but again are fully reversible. It appears likely that hydrogen from the organic binders could diffuse into the crystal in this case; our observations are consistent with this interpretation.

A common denominator in all the above results is the critical dependence of room temperature dielectric loss on any heat treatments given the sample during or after application of electrodes. Heating to 100°C for a few minutes frequently resulted in changes in D by factors of two or more, and minor changes were even observed after "annealing" at room temperature. In general, large loss peaks were observed in crystals heated to 250°C or more, then rapidly cooled to room temperature. Prolonged annealing at temperatures below 250°C or slow cooling (~10°C/hr or less) resulted in low loss, although results depended strongly on ambient during heat treatment, sample purity, and thermal history.

Because of the irreversible changes with other electrode materials, the remainder of our discussion will be confined to results obtained with Ag and Au electrodes. "Typical" results for a nominally stoichiometric crystal ($\rho \gtrsim 10^{13}$ Ω cm, as inferred from two terminal dc conductivity measurements) at room temperature are presented in Fig. 4,

in terms of C/C_o (where C is the measured series equivalent capacitance and C_o is the calculated capacitance for a loss-free crystal, assuming $\epsilon/\epsilon_o = 173$). The crystal was 500μ thick, had been carefully lapped and etched to remove surface damage, and annealed in air at 800°C. Ag electrodes were applied at room temperature; the measured dissipation and capacitance are shown as Curves A in Fig. 4. Subsequent heat treatment (with electrodes in place) for 12 hours in air at 350°C, followed by rapid cooling to room temperature resulted in Curves B. The striking changes in C and D are fully reversible; repeating the 350°C heating cycle after removal of electrodes restored the behavior indicated by Curves A. It was not always possible to achieve the low loss indicated by Curves 4A; however, alternate heat treatment with and without electrodes always produced large changes in C and D, which were reproducible for many cycles. Heating to lower temperatures with electrodes and quenching results in a shift of the dissipation peak to lower frequency and a decrease in peak height, as would be predicted by the analysis in Sec. II.

As previously noted, the observed results are strongly dependent on a number of experimental parameters; these curves should only be viewed as representative of results obtained for the conditions specified.

A few measurements were made at temperatures intermediate between room temperature and annealing temperature. The parameters (C and D) generally were quite unstable, as would be expected. The results were in qualitative agreement with predictions of the analysis of the preceding section.

D. Effect of Ambient During Heat Treatment

The dissipation curves observed for a given heat treatment of a particular crystal were found to depend strongly on the atmosphere in which the treatment was carried out. The results obtained appeared to depend only on the equivalent H_2 partial pressure of the atmosphere and could in all cases be interpreted at least qualitatively in terms of the analysis of the preceding section, by assuming that the migrating donors were H^+ interstitials and that the equilibrium H^+ concentration in a given crystal was determined by the equivalent H_2 pressure in the ambient. Among the ambients tested (in order of increasing H_2 partial pressure) were O_2 (with liquid nitrogen cold trap), O_2 (saturated at room temperature with H_2O) pure H_2O vapor, NH_3-H_2O, and pure H_2 ($\rho \leq 0.01$ Torr). The general behavior for crystals quenched from a given annealing temperature in various H_2 partial pressures was for the dissipation peak to shift to higher frequencies with increasing H_2 pressure, as would be expected from a raising of the Fermi level in the crystal. Thus, atmospheres with very small partial pressures of H_2 generally resulted in loss peaks at low frequency; often the peak appeared to be below the experimentally accessible range and only a low frequency "tail" was observable.

One important exception to this behavior was observed. A 250μ $c_\perp$ crystal of relatively high purity (no quantitative information available) was etched and strongly oxidized (O_2, 100 Torr, with liquid nitrogen cold trap, 40 hours at 950°C, slow cooled) before applying Au electrodes. Subsequent heat treatment in dry O_2 at 350°C produced a large loss peak at $\sim$ 5 kHz, which shifted to lower frequency and disappeared at successively higher H_2 partial pressure. D was < 0.01

over the frequency range from 20 to 10^5 Hz after heating in 20 Torr of H_2O. Further increase in H_2 pressure resulted in the usual behavior (a loss peak moving to higher frequencies as P_{H_2} increased). This is strongly suggestive of p-type behavior (which has not previously been convincingly demonstrated in TiO_2), produced by a Fermi level near the top of the valence band in the bulk of the crystel, with an insulating layer beneath the electrodes resulting from n-type electrode contact.

The H interstitial concentration in these crystals was independently monitored by observation of the infrared absorption associated with the OH stretching vibration.[14] Although the concentration was strongly sample-dependent (presumably due to variation in electron trap density), the results were consistent with the interpretation above, in that the H concentration increased monotonically with increasing H_2 partial pressure of the annealing atmosphere. Measured H concentration ranged from $\sim 5\times10^{17}$ to $10^{19}/cm^3$ for the various atmospheres described above. This is a surprisingly narrow range of concentrations in view of the fact that P_{H_2} (H_2 partial pressure in the ambient) changed by many orders of magnitude (the equivalent P_{H_2} in a dry O_2 atmosphere is undoubtedly determined by outgassing of hydrocarbons from o-rings, etc., but is unlikely to be larger than 10^{-20} Torr). However, this weak dependence on P_{H_2} is readily accounted for in a crystal such as rutile by an analysis of the thermodynamics of the process. It is readily shown that

$$n_{H^+} \propto (P_{H_2})^{1/4} e^{- E_F/2KT}$$

where n_{H^+} is concentration of H^+ interstitials and E_F is the electron Fermi level in the crystal. E_F may change by an amount comparable to the band gap ($\sim$ 3.2 eV in TiO_2) as n_{H^+} is varied, if there is some

concentration of deep electron trapping levels in the crystals, and H^+ is the dominant donor impurity. This readily accounts both for the limited solubility of H^+, even in a pure H_2 atmosphere, and the extreme difficulty in reducing n_{H^+} below $\sim 10^{17}/cm^3$. The strong dependence of H^+ solubility on E_F probably also accounts for the difficulty in making meaningful measurements of H^+ diffusion in TiO_2.

The observed dependence of P_{H_2} appears to establish the H^+ interstitial as the required mobile impurity in at least some cases. Whether or not it is the only mobile ion is a question which cannot be answered on the basis of presently available results. The possibility of other ions (particularly Tl^{44}, which is known to be present in substantial concentrations)[16] participating in the process cannot be ruled out. The equilibrium configuration for two or more mobile ions is likely to be quite complicated, due to the dependence of solubility on electrostatic potential discussed above. The rather surprising results obtained from calculations for the single ion case suggest that the resistivity profile resulting from redistribution of several ion species could be very complex.

E. Voltage Dependence of Measured Dissipation

In most cases, the measured dissipation was essentially independent of the amplitude of the ac voltage applied to the crystal, at least up to $\sim$ 30V rms. The results described above refer only to such cases, or to crystals for which the measured dissipation was constant for sufficiently small applied voltage. In some crystals, however, a striking voltage dependence of both capacitance and dissipation was observed. These were crystals which had been equilibrated in rather high partial pressures of H_2, presumably resulting

in a Fermi level fairly near the conduction band. In some cases, the dissipation at low frequencies ($\lesssim 10^3$ Hz) was observed to change by as much as a factor of 10 as the applied voltage was increased in the range from 1 to 30 volts rms. A similar voltage dependence of the apparent dc conductivity was also observed. This effect is not to be confused with the time-dependent conductivity frequently observed in rutile,[17] which is presumably due to field-induced ion motion. Some minor changes in our observed conductivity occurred several hours after applying a dc field, but the effect described here was clearly different, since changes in conductivity occurred on a millisecond time scale. As the frequency was increased, the voltage dependence of D diminished and was essentially unobservable at 10^5 Hz at voltages up to 100 volts. The observed behavior is well represented by an equivalent circuit consisting of an ideal loss-free capacitor (with c equal to the calculated capacitance of the crystal), in parallel with a voltage-dependent resistor. Interestingly, the frequency below which D increased substantially above the small signal level at a given voltage corresponded approximately to the reciprocal of the transit time for an electron, predicted from the applied voltage and observed carrier mobility (~ 0.3 cm^2/volt sec).[3] This appears to imply that it is possible for carriers to be injected at one electrode, and travel completely through the specimen without being trapped--which would be surprising to say the least.

IV. Conclusions

It is difficult to draw many firm conclusions from the admittedly qualitative results presented here. However, the results are sufficiently interesting and suggestive to merit a tentative interpretation.

Part of the observed behavior--the enhancement of dissipation which results from heating and quenching of a crystal with electrodes--appears to be at least qualitatively explained by the electronic loss mechanism outlined in Sec. II, which we believe has not been previously suggested. It seems likely that this loss mechanism may be fairly common in insulating crystals, particularly in the titanates, and in other transition metal oxides. Similar though less dramatic observations have been reported in Al_2O_3 and MgO,[18] neither of which are particularly good candidates for such a mechanism, because of their large band gap and small ϵ. Other observations, such as the dependence of observed loss on heat treatment prior to electrode application, sample purity, and surface damage, cannot be accounted for in detail at present, but are probably the result of known mechanisms.

However, some of our observations do not appear to be consistent with current understanding of this crystal, and merit much closer examination. Of particular interest, because of the apparent implications, are 1) the voltage dependence of D observed in some cases, and 2) the large loss in some heavily oxidized crystals, which first decreases, then increases again after heating in successively higher P_{H_2}.

APPENDIX A

The method chosen employs the Tchebycheff technique for numerical integration. This is, of course, not the only possible approach and in some of our cases not the best. It is the simplest and has proven adequate for our purposes.

In the Tchebycheff method of numerical integration, the integral is approximated by:

$$\int_{-\frac{1}{2}}^{\frac{1}{2}} \phi(u)du = \frac{1}{n}\left[\phi(u_1) + \phi(u_2) + \text{---} + \phi(u_n)\right]$$

where the u_i are the zeros of the Tchebycheff polynomials. This formula can be extended to an arbitrary range of integration by a transformation of variables:

$$\int_a^b y(x)dx = (b-a)\int_{-\frac{1}{2}}^{\frac{1}{2}} \phi(u)du$$

where:

$$x = (b-a)u + \left(\frac{a+b}{2}\right)$$

$$\phi(u) = y\left[(b-a)u + \left(\frac{a+b}{2}\right)\right]$$

Hence the expression for $D(\omega)$ becomes:

$$D(\omega) \approx \frac{\sum_{b=1}^{n} \dfrac{\rho_b}{(\rho_b \omega \epsilon)^2 + 1}}{\sum_{b=1}^{n} \dfrac{\rho_b^2 \epsilon \omega}{(\rho_b \omega \epsilon)^2 + 1}}$$

We then form the function

$$\Psi = \sum_{j=1}^{n} (\log \hat{D}_j - \log D_j)^2$$

where $\hat{D}_j$ is the measured dissipation and D_j the calculated dissipation

at $\omega = \omega_j$. We then choose the set ρ_k to minimize ψ. A computer program has been written to accomplish this. It calculates the required change in the set ρ_k assuming the original set, ρ_k, is close enough to the minimum for a quadratic fit to be accurate. It then calculates the gradient and makes a step whose length and direction is a compromise between the quadratic and gradient methods. The relative weight given each is determined by the angle between the two directions, i.e., when the angle is large the gradient method is heavily weighted. Once the optimum set ρ_k is determined, it is plotted against the roots of the Tchebycheff polynomials to obtain the resistivity spectrum.

References

1. F. A. Grant, Rev. Mod. Phys. 31, 646 (1959).
2. A. von Hippel, J. Kalnajs and W. Westphal, J. Phys. Chem. Solids 23, 779 (1962).
3. G. A. Ackett and J. Volger, Physica 32, 1680 (1966).
4. L. E. Hollander and P. L. Castro, J. Appl. Phys. 33, 3421 (1962).
5. R. A. Parker, Phys. Rev. 124, 1719 (1961), and R. A. Parker and J. H. Wasilik, Phys. Rev. 120, 1631 (1960).
6. J. Maserjian and C. A. Mead, J. Phys. Chem. Solids 28, 1971 (1967).
7. K. G. Srivastava, Phys. Rev. 119, 516 (1960).
8. G. J. Hill, Brit. J. Appl. Phys. 1, 244 (1968).
9. We may approximate the behavior of a given layer as that of a simple parallel RC circuit. This element alone would exhibit a monotone decreasing dissipation as frequency increases. However, if it is "in series" with other layers of higher resistivity and equal or greater thickness, its total impedance will be small compared to the other elements at frequencies $\omega \ll \frac{1}{RC}$. Thus, both high and low resistivity layers are required to produce a peak in D vs ω. Under these circumstances, a given layer contributes significantly to the dissipation only at frequencies near $\omega = \frac{1}{RC} = \frac{1}{\rho\epsilon}$.
10. W. Schmidt, Ann. Phys. 9, 919 (1902) and 11, 114 (1903).
11. J. M. Ziman, Principles of the Theory of Solids (Cambridge Univ. Press, 1964), p. 139.
12. O. W. Johnson, Phys. Rev. 136, 284 (1964).
13. Paul I. Kingsbury, Jr., W. D. Ohlsen and O. W. Johnson, Phys. Rev. 175, 1099 (1968).

14. O. W. Johnson, W. D. Ohlsen and Paul I. Kingsbury, Jr., Phys. Rev. 175, 1102 (1968).

15. The question of work functions in insulating crystals, as well as much of the material in the preceding paragraphs is discussed in Mott and Gurney, Electronic Processes in Ionic Crystals (Oxford Univ. Press, 1950), Chap. 3.

16. Paul I. Kingsbury, Jr., W. D. Ohlsen and O. W. Johnson, Phys. Rev. 175, 1091 (1968).

17. O. W. Johnson, Appl. Phys. Letters 13, 338 (1968).

18. N. M. Tallan and D. P. Detwiler, J. Appl. Phys. 34, 1650 (1963).

19. J. B. Scarborough, Numerical Mathematical Analysis, 4th Edition (Johns Hopkins Press) Chapter 7.

Figure Captions

1.

a) Assumed band configuration of isolated rutile, and metal electrode.

b) Band configuration of system after electrical contact is established.

2.

Location of conduction band minimum relative to Fermi level vs position in crystal, with metal electrode at x = 0. Curve A is initial configuration at room temperature. Curve B is the calculated equilibrium configuration at 350°C, after ion migration. Curve C is the corresponding configuration after quenching to room temperature.

3.

Calculated room temperature capacitance and dissipation for band configurations in Fig. 2. Curves A (this figure) corresponds to Fig. 2A, curves B correspond to Fig. 2C. C_o is the calculated (loss-free) capacitance assuming $\epsilon = 173\ \epsilon_o$.

4.

Measured room temperature capacitance and dissipation for crystal described in text. Curves A were obtained before heat treatment, curves B after equilibrating at 350°C in air and quenching to room temperature.

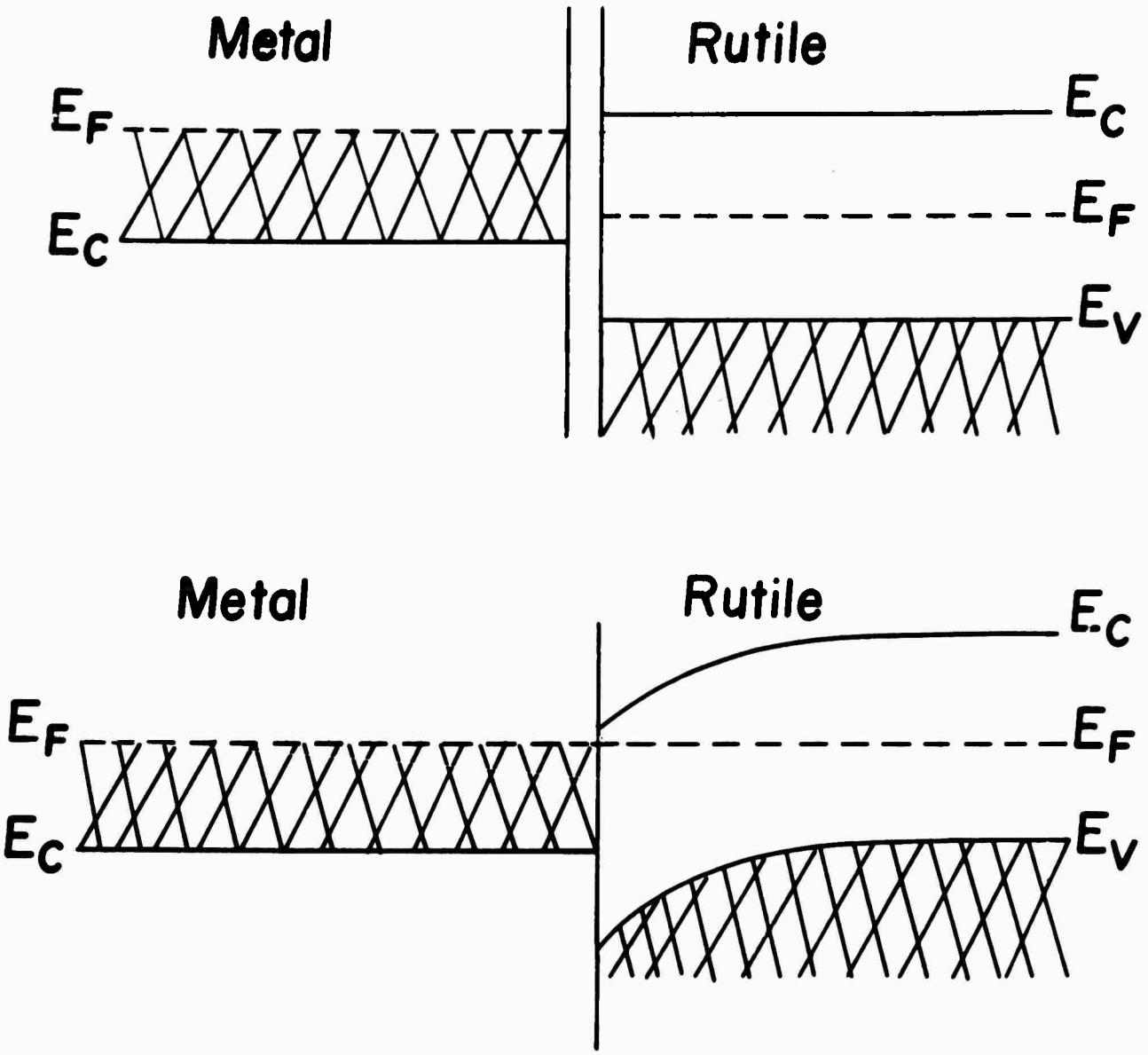

Fig. 1

a) Assumed band configuration of isolated rutile, and metal electrode.

b) Band configuration of system after electrical contact is established.

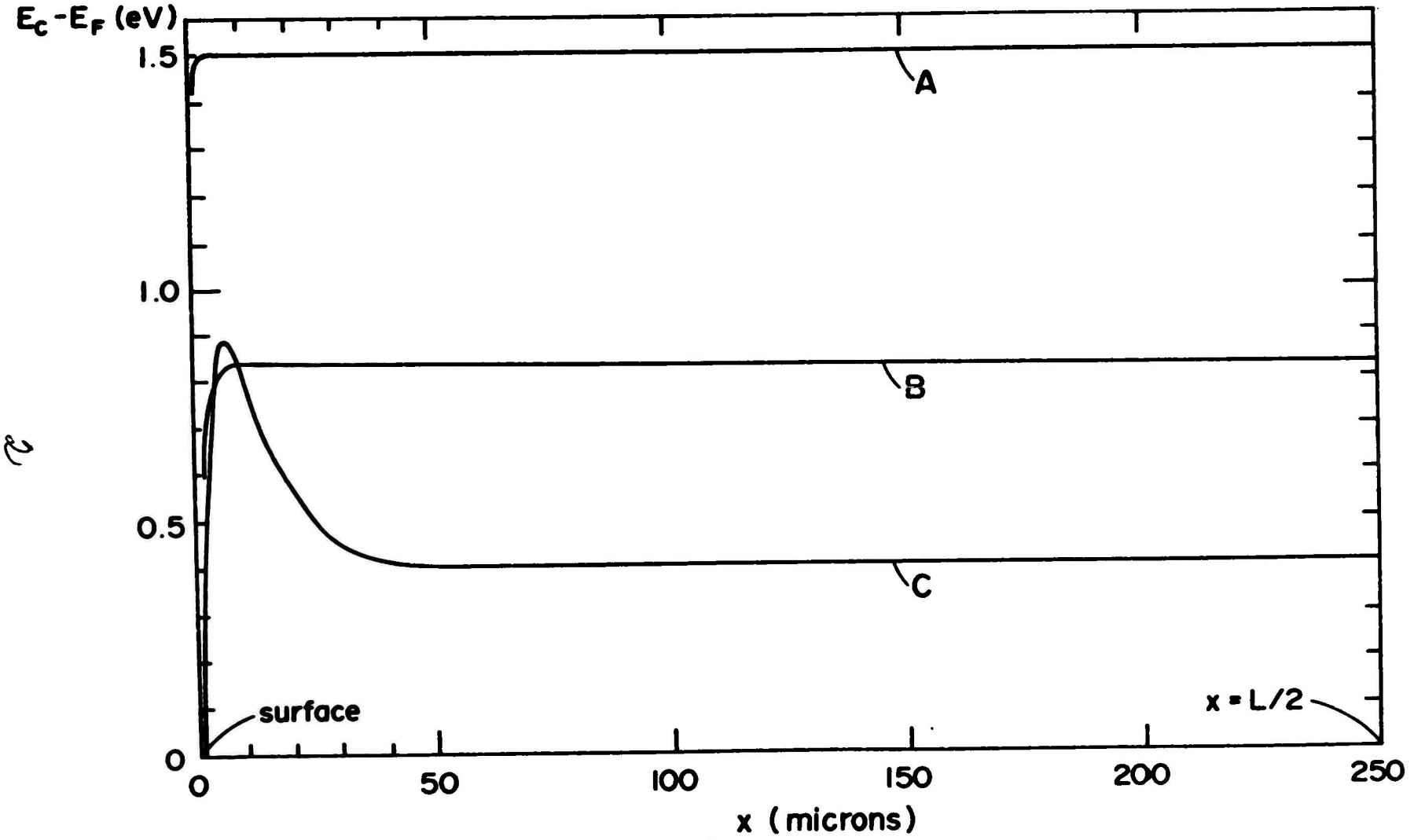

Fig. 2

Location of conduction band minimum relative to Fermi level vs position in crystal, with metal electrode at x = 0. Curve A is initial configuration at room temperature. Curve B is the calculated equilibrium configuration at 350°C, after ion migration. Curve C is the corresponding configuration after quenching to room temperature.

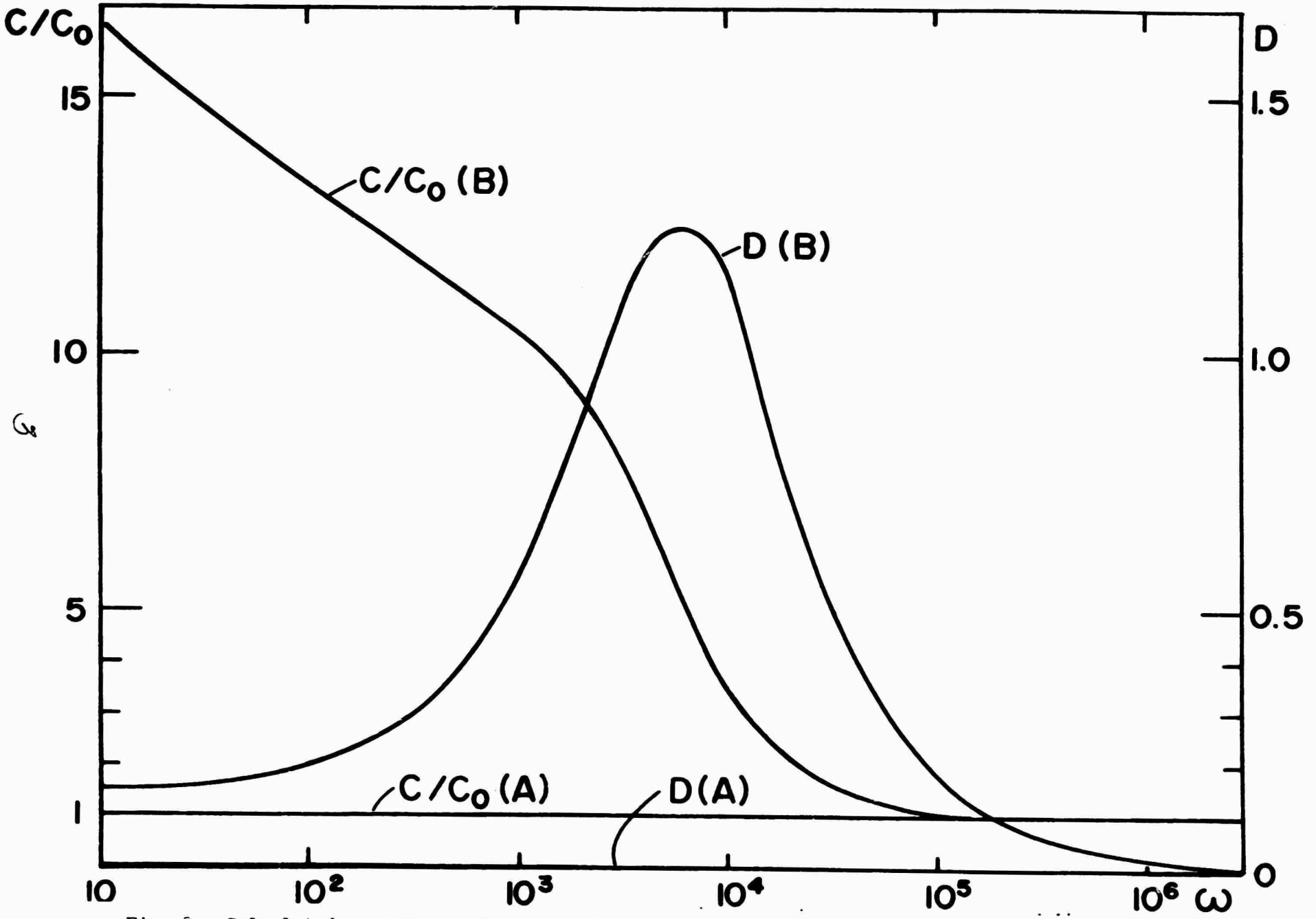

Fig. 3 Calculated room temperature capacitance and dissipation for band configurations in Fig. 2. Curves A (this figure) correspond to Fig. 2A, curves B correspond to Fig. 2C. C_o is the

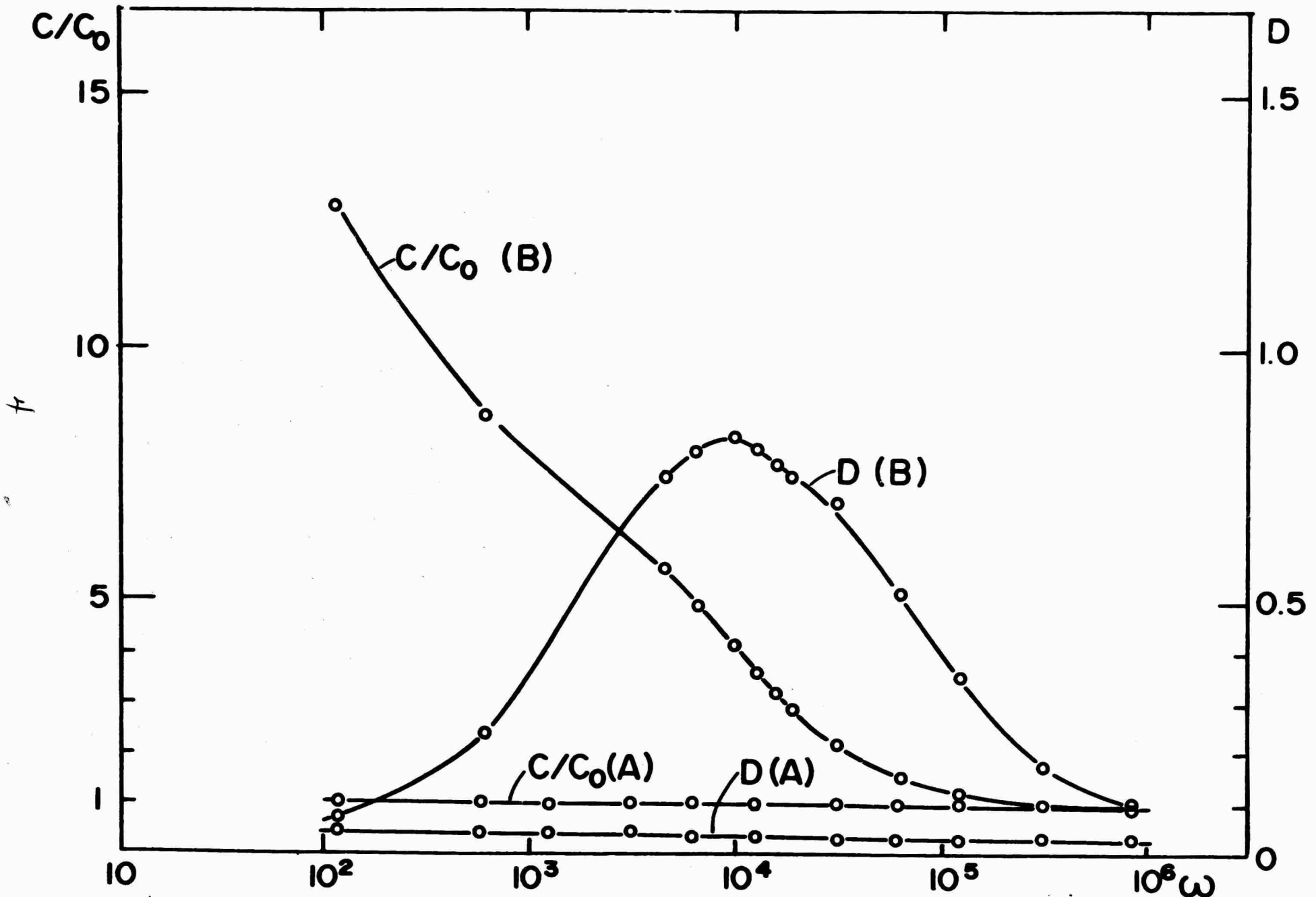

Fig. 4 Measured room temperature capacitance and dissipation for crystal described in text. Curves A were obtained before heat treatment, curves B after equilibrating at 350°C in air and quenching to room temperature